Chapitre 3

Bacterial flagella grow through an injection-diffusion mechanism

3.1 Avant-propos

L'idée de ces expériences est venu en observant la quantité incroyable de données disponibles découlant des manipulation décrites au chapitre précédent. En effet, la très grande majorité des filaments présents sur la lame de microscopes n'étaient pas coupés et subissaient un double marquage. J'ai de plus remarqué de façon très qualitative que la longueur des bouts marqués en deuxième semblaient plus courts lorsque les premiers bouts étaient long et vice-versa. Nous avons donc décidé de faire une étude plus complète de ces données en ajoutant des souches spéciales contenant des protéines de flagelline modifiées permettant de tester l'hypothèse qu'une chaîne de protéine est le méchanisme régissant la croissance du filament. Nos données ont dès le départ montré une dépendance du taux de croissance avec la longueur du filament pour toutes les souches étudiées. Comme nous voulions nous assurer que les filaments ne se brisaient pas ou que la bactérie de mourrait pas, j'ai mis au point une technique de marquage triple unique qui assurait la qualité des résultats obtenus. Comme au chapitre précédent, ces résultats vont à l'encontre d'un modèle proposé dans *Nature* sur le mécanisme d'assemblage du filament. Ce modèle repose sur l'hypothèse que la longueur du filament croit à vitesse constante, peu importe sa longueur. Nos résultats montrant un taux de croissance qui diminue avec la longueur du filament tendent donc vers un modèle différent décrivant ce mécanisme de croissance.

Le groupe de recherche du Dr. Erhardt a alors débuté les mêmes expériences en les répétant sur d'autres souches de bactéries. De plus, un groupe de recherche japonais travaillait au même moment sur un projet parallèle et leurs résultats complétaient les nôtres. Un article incluant plusieurs autres expériences fut écrit en collaboration avec ces groupes de recherche. Le travail réalisé fut monumental et les conclusions importantes pour permettre de proposer un nouveau

modèle sur l'assemblage du filament bactérien. Cet article a été soumis au magazine *eLife* et a été accepté pour publication (L'article a été publié le 6 mars 2017[65]). Les résultats que j'ai obtenus se sont donc retrouvés dilués au sein de la foule de données présentée dans l'article. Le but de cette thèse étant de décrire les expériences et résultats que j'ai obtenus lors de mon doctorat, ce chapitre présente donc exclusivement les résultats que nous avons amassés dans notre laboratoire.

À l'origine, nous avions en tête de publier ces travaux séparément avant de tout regrouper en un seul article. Pour cette raison, il a été rédigé en anglais. J'ai donc décidé de le garder dans cette langue et dans un format article pour en conserver le ton original. Ce chapitre contient donc l'entièreté des résultats découlant des expériences que j'ai réalisées dans le cadre de ce doctorat. Comme les conclusions de ce chapitre se basent aussi sur les résultats obtenus et les analyses réalisées par nos collaborateurs, le manuscrit de l'article complet se retrouve à l'annexe B.

3.2 Résumé

Plusieurs types de bactéries peuvent se déplacer dans leur milieu à l'aide de flagelles rotatifs. Les filaments flagellaires peuvent atteindre plusieurs fois la longueur du corps à l'extérieur de la cellule. Ceux-ci sont composés d'un assemblage de plusieurs milliers de protéines identiques appelées flagelline. Ces flagellines sont exportées dépliées dans un canal de sécrétion et sont assemblées à l'aide d'une protéine agissant comme bouchon au bout du filament. Dans ce chapitre, nous étudions le taux de croissance de ces filaments en fonction du temps. L'assemblage de filaments individuels fut observé directement et leur longueur fut précisément mesurée à l'aide de multiples marquages fluorescents. Deux souches inhibant la formation de chaînes de protéines dans le canal central furent aussi utilisées. Les résultats obtenus montrent une diminution du taux de croissance en fonction de la longueur du filament. Les souches inhibant la formation de chaînes de protéines dans le canal central présentent le même comportement ainsi qu'un taux d'assemblage similaire aux souches de type sauvage. En combinant nos résultats à ceux obtenus par différents groupes collaborateurs, nous proposons un modèle décrivant l'assemblage de filaments s'appuyant sur un mécanisme d'injection-diffusion

3.3 Abstract

Many bacteria swim by rotating long appendages called flagella. Flagellar filaments are assembled from thousands of subunits that are exported unfolded through a secretion channel and added at the tip of the filament with the help of a capping protein. In this work, we are looking at the rate of growth of the filament as a function of time. The assembly of individual filaments was directly observed and the length of each segment was precisely measured using multiple fluorescent labelings. Two strains were also used that would inhibit the formation of

a chain of subunits in the central channel. The results described in the following work show a decrease in the rate of growth of the filaments in function of its length. The strains inhibiting the formation of a chain of subunits show the same trend as well as rates of growth similar to wild type strains. In addition with similar work done by collaborating groups, we propose a model for the assembly of flagellas that rely on an injection-diffusion mechanism.

3.4 Introduction

The bacterial flagellum is a nanomachine, which self-assembles several tens of thousands flagellin subunits outside the cell, where no discernible energy source is available. Elongation of flagellar filaments is remarkably fast with up to ∼1,700 amino acids (∼3.5 flagellin subunits) secreted and assembled per second. A fundamental problem concerns the molecular mechanism of how the long external filament self-assembles at such a rapid rate outside the cell. Here, we monitored the dynamic assembly of individual flagella using *in situ* labeling and real-time imaging of elongating flagellar filaments. We demonstrate that the rate of filament elongation decreases with length and follows an injection-diffusion mechanism. Putative head-to-tail subunit interactions inside the filament channel, previously proposed to explain the mechanism of flagellum growth, did not contribute to the filament elongation dynamics. Inhibition of the proton motive force dependent protein export decreased the flagella growth rate to be virtually length independent as predicted by the injection-diffusion model[1]. These findings illustrate that a simple, diffusion-based mechanism controls bacterial flagella growth outside the cell.

Many bacteria move by rotation of a helical organelle, the flagellum. The external flagellar filament is several times longer than a bacterial cell body and is made out of up to 20,000 flagellin subunits[66, 13, 16, 67] (Fig. 1a[2]). A type III export apparatus located at the base of the flagellum utilizes the proton motive force (pmf) as the primary energy source to translocate axial components of the flagellum across the inner membrane[15, 14, 68, 69]. Exported substrates travel through a narrow 2 nm channel within the structure and self-assemble at the tip of the growing flagellum. It has been a mystery how bacteria manage to self-assemble several tens of thousands protein subunits outside the cell, where no discernible energy source is available. Previous reports in the literature concerning the mechanism of flagellum growth have been conflicting[47, 70, 48, 71]. An exponential decay of filament elongation with length was observed using electron microscopic measurements, which was proposed to be a result of decreased translocation efficiency[47, 72]. Turner and al. used fluorescent bi-color labeling of flagellar filaments to measure filament growth in *Escherichia coli* in a population-approach[48]. They used differential fluorescent labeling of flagellar filaments to distinguish new filament growth from old filament growth and concluded by measuring the length of hundreds of filaments that the growth of filaments is independent of their length. A model based on the pulling

1. Expériences et résultats situés dans l'Annexe B
2. Voir Annexe B

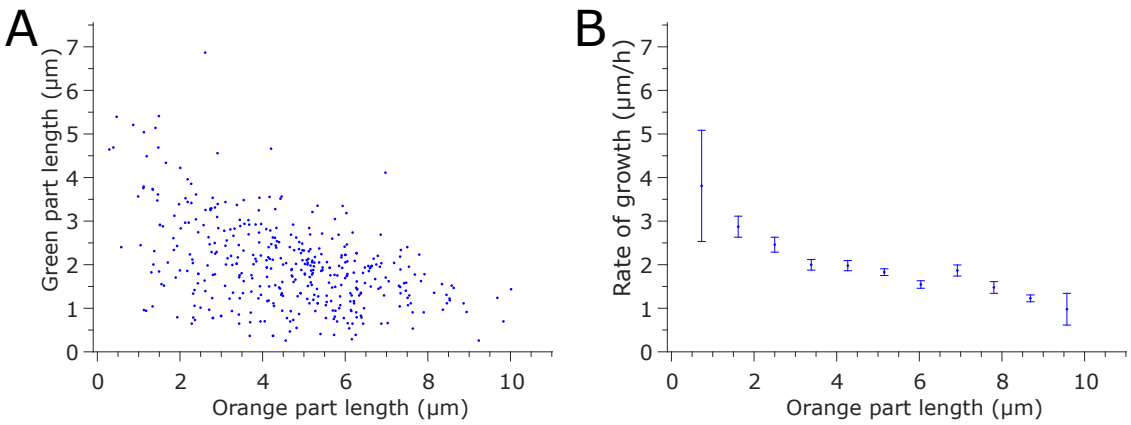

FIGURE 3.1 – Rate of growth of filaments in EM800 strain.381 different filaments were measured and graphed in A. The mean of bins 0.89 µm wide was computed and graphed in B to show the decline in rate of growth. The error bars are the standard deviation of the distribution of each bin.

force of a filament-spanning chain of flagellin subunits was proposed to explain the apparent length-independent growth[71].

3.5 Results

3.5.1 Bicolor labeling

A total of 381 bicolor filaments were recorded with the strain EM800 and were plotted with the green part in function of the orange part (Fig. 3.1A). Every points represents a orange filament with a green part that had 1 hour to grow at 37°C. Orange segments without green part were not taken into account possibly indicating cell lysis. Since green-only segment show new filaments growing only during the second growth period, the time when they started growing could not be determined and they were not considered in the analysis. The different length were binned and the mean was computed for each bin. Fig 3.1B shows the graph of those means. The number of bins was determined using a Matlab function which combine 3 different methods of determining bins and taking the mean of those 3.

2 strains were developped to determine whether a chain of FliC could be formed in the central channel of the filament as proposed by Evans and al.[71]. When Arabinose is absent, the strains behave exactly like EM800. When the promoter is added, they express fusion proteins of a flagellar substrate with an unrelated C-terminal protein domain (beta-lactamase). This means that if a chain of fliC can occur, the presence of arabinose would break that chain in the central channel of the filament.

Fig. 3.2 shows the average plots of each strain with and without the presense of arabinose. Scatter plots for each strain are available in Supplemental Material. The averages were obtai-

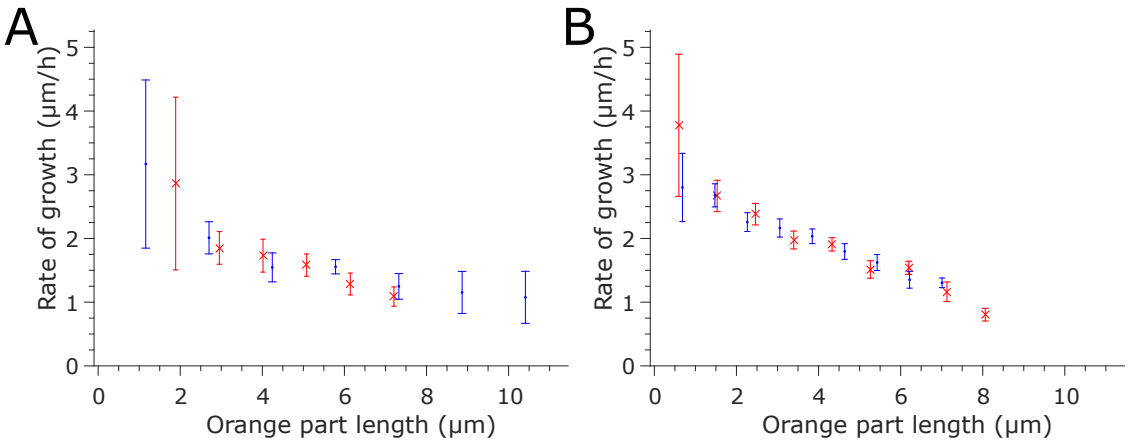

FIGURE 3.2 – Rate of growth of EM1281/1282 strains with and without arabinose. A shows strain EM1281 and B strain EM1282. Red 'x' markers show filaments which have not grown in presence of arabinose while blue '.' markers show filament which grew in the presence of arabinose. The data points were obtained by averaging the lengths of bins obtained in similar way as for EM800 strain. The error bars are the standard deviation of the distribution of each bin.

ned using the same method as the EM800 strain. One would expect a clear difference between the plots with and without the promoter if a chain of flagellar substrates was formed in the central channel of the filament. However we can't see a clear trend as the 2 graphs show the same downward trend with a same growth rate. Since those 2 strains without arabinose behave like EM800, we would also expect a similar behavior. By comparing Fig. 3.1 and Fig. 3.2, we can see a similar pattern a decreasing growth rate versus initial length.

Similar experiments were done with a wild-type strain (EM2011). Fig. 3.3 shows the results obtained with 255 filaments measured. Experiments in the presence of arabinose were also conducted as a control and results are in the supplementary material.

3.5.2 Tricolor labeling

To ensure that the second part did not stop growing during the 1-hour period, we also performed 3-color labeling. The order of labeling was changed however since for an unknown reason, the labeling with AF546 in the cell gave enourmous backgroung noise compared to the fluorescent signal of the filaments. Hence, we performed the first 2 rounds of labeling in the tube and only the third one was done in the cell. A graph of the results of 122 filaments is shown in Fig. 3.4. Only filaments with 3 distinct segments are shown in the graph. A graph of filaments with only the 2 first segments and lacking a third one is available in the supplementary material.

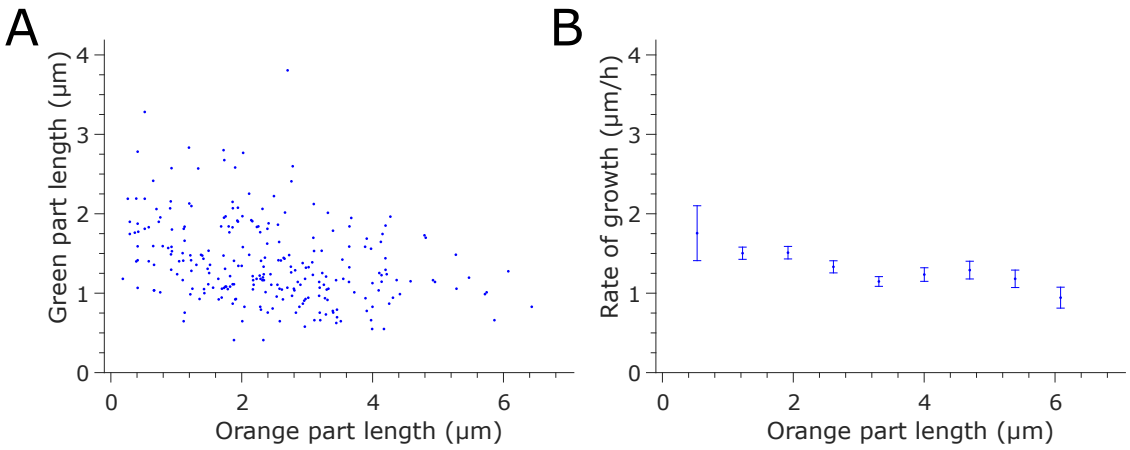

FIGURE 3.3 – Rate of growth of filaments in EM2011 strain. 255 different filaments were measured and graphed in A. The mean of bins obtained the same way as the EM800 strain was computed and graphed in B to show the decline in rate of growth. The error bars are the standard deviation of the distribution of each bin.

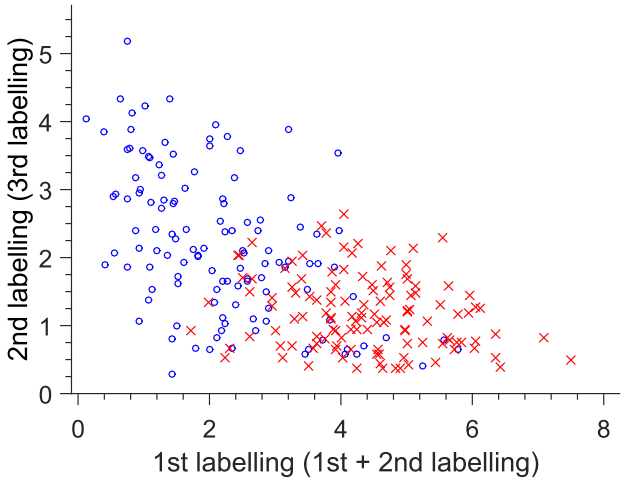

FIGURE 3.4 – Rate of growth of filaments in EM2011 strain using triple labeling. Blue 'o' markers show the length of the second labeling in function of the length of the first labeling. Red 'x' markers show the length of the third labeling in function of the length of the first and second labelings added. Each point on this graph had 3 distinct segments. Filaments with only 2 segments are not shown here.

3.6 Discussion and Conclusion

This study focused on the rate of growth of bacterial filaments as a function of its length. A previous study by Turner and al. [48] found that *E.coli* filaments' rate of growth was independent of its length. Those results were used by Evans and al. [71] to suggest a chain mechanism model for the growth of bacterial filaments. By looking at the graphs of the length of filaments and especially the graphs of the means, we can clearly see a downward trend in the rate of growth which is in contrast to Turner and al. [48]. Since our initial experiments were done using a modified strain missing part of the flagellar motor (EM800), we did it again with a wildtype strain (EM2011) in which we saw a slower rate of growth, but a downward trend nonetheless.

To further our investigation of the chain model, 2 strains were modified to have a secreted protein with an unrelated C-terminal at the end of it. Those specific substrates would be secreted only in the presence of the promoter arabinose. Those unrelated terminal (FlgL-bla and FlgM-bla for EM1281 and EM1282 respectively), when secreted, prevent the formation of a chain of FliC. Those two substrate continue to be secreted by the bacteria and excreted through the filament's central channel by the export apparatus during the growth of the filament [47]. Since FliC is secreted much more than those two substrates, we would expect a slowing down of the rate of growth be it dependent or independent of its length since the presence of either FlgL-bla or FlgM-bla would break a proposed chain. Without the presence of arabinose, the normal substrates FlgL and FlgM are secreted and the strains behave exactly like EM800.

We can see in Fig. 3.2A and B that the rate of growth decreases in a similar fashion as EM800 whether arabinose is present or not which should not be the case is a chain of protein was present. We would expect the blue '.' marker to be lower on the graph indicating a slower rate of growth. However, we see that even when the unrelated C-terminal substrates are secreted, the rate is the same in both strains with and without arabinose. We thus conclude that the proposed chain mechanism model might not explain exactly what is happening.

Finally, since our results are so different from [48], we wanted to be sure that we did not measure length of dead filaments. To do so, we repeated the same experiments, but we added a third period of growth with a third labeling. This ensures the filament grew for the whole hour during the second period of growth. We can see in Fig. 3.4 that there is still a downward trend in the rate of growth of the second part versus the first one. The red 'x' marker show the third labeling versus the previous two added together. Of course, like in the bicolor case, we cannot say that all filament grew for the whole hour but, nonetheless, we can see a clear downward trend.

This change in the rate of growth in incompatible with a chain mechanism for the building of the filament. With the seemingly exponential decay in the rate of growth we could be tempted

to go for diffusion of unfolded proteins as the main mechanism for flagellar building. However, since the decrease of rate does not go to zero, but it rather stabilizes at around 1 µm/h, there must be a driving force in the export apparatus of the motor. More experiments were conducted by collaborators who independently observed the same trend of decreasing rate of growth as the filament grow longer. Moreover, experiments inhibiting the pmf of the bacteria were conducted which showed that the rate of growth was slowed down by the absence of the pmf. Considering these results in conjunction with ours, we proposed an injection-diffusion mechanism for the bacterial flagellar growth.

3.7 Materials and Methods

3.7.1 Strains and growth

The *Salmonella enterica* serovar Typhimurium (*Salmonella* Typhimurium) strains used in this study are listed in table 3.1 in the Supplementary Material. The generalized transducing phage of *Salmonella* Typhimurium P22 *HT105/1 int-201* was used in all transductional crosses[61]. Strains were streaked from frozen stock (-80°C) on bacterial plate (10 g Bacto tryptone, 15 g Bacto agar and 5 g NaCl per liter). An isolated colony was inoculated in 10 ml TB broth (10 g Bacto tryptone and 5 g NaCl per liter) in 125 ml Erlenmeyer flask and placed at 34°C for 15 hours with gyration at 200 rpm. A volume of 100 µl of the saturated culture was inoculated in 10 ml TB broth in 125 ml Erlenmeyer flask and placed at 34°C for 4h with gyration at 200 rpm, until it reached an $OD_{600} \approx 0.45$ ($\sim 4 \times 10^8$ cells/ml). The culture was centrifuged for 5 minutes at $1,500 \times g$ and gently resuspended in 100 µl motility buffer (MB) (0.01 M potassium phosphate (pH 7,0), 10^{-4} M EDTA).

3.7.2 Labeling and microscopy

The first labeling was done by adding 5 µl of Alexa-Fluor maleimide 546 dye (A-10258, Life Technologies) to the 100 µl MB (0.5 mM) and was left in the dark at room temperature for 1 hour. This dye was chosen for a selective labeling of the cystein-modified fliC. The dye was washed by adding 10 ml of MB and centrifuge the tube for 5 minutes at $1,500 \times g$ twice. A custom-made flow-cell was fabricated using a standard microscope slides (25 × 75 mm) and a 18 × 18 mm coverslip (cleaned with 70% ethanol). Two stripes of Parafilm were placed ∼1 cm apart between the slide and coverslip and gently pressed after heating over a flame in order to form a tunnel. A drop of Poly-L-lysine 0,01% (Sigma) was left on the coverslip for 5 minutes and then rinsed before the flow-cell was fabricated. This tunnel was then filled with 50 µl of cell suspension and left 10 minutes upside-down for the cells to deposit and stick to the coverslip. Cells that were still in suspension were rinsed away with 200 µl of motility buffer (MB).

A second labeling was then performed with a different dye : Alexa-Fluor maleimide 488 (A-

10254, Life Technologies). During that second labeling, the dye was diluted to 1 mM in LB broth (10 g Bacto tryptone, 5 g yeast extract and 5 g NaCl per liter) and the cell was left in the dark humidity chamber at 37°C for 1 hours. To overexpress the fusion proteins breaking a proposed chain of flagellar substrates, arabinose was added to the LB broth during the second labeling to a final concentration of 0.2%. The excess dye was washed by gently flowing 600 µl of MB, and the filaments could then be observed in fluorescence microscopy (Olympus, IX71). The cell was filled with Poly-L-lysine 0,01% to stop flagellar rotation and have the filaments stick to the cover-slip. Once the flow-cell was positionned, a high-numerical-aperture objective (Olympus, 100x, 1.3 NA) was used for imaging. Images in fluorescence were taken of different fields in the same flow-cell for analysis using a EMCCD camera (iXon 888, Andor Technology, Northern Ireland).

For the triple labeling assays, things had to be done differently since, for an unknown reason, labeling with AF546 in the cell gave huge background noise compared to the signal of the labelled filaments. Therefore, after the first labeling was done the same way as before except with AF488, the culture was resuspended in 2 ml of LB and put in the incubator for 1 hour in the dark. After centrifuging the tube for 5 minutes at $1,500 \times g$, bacteria were resuspended in 100 µl of MB for the second labeling with AF546. The rest of the procedure was done the same way as before.

3.7.3 Image analysis

Images were analysed using ImageJ software. Each color of fluorescence were combined (ovelayed) to form a single image with both colors. Using different lookup tables, bicolor filaments could be seen on the image (see Fig. 2.4 for an example).

Images were loaded in ImageJ with the plugin NeuronJ. Each filament was traced manually with an automatic help from the plugin. Vertices of the traced segments were ajusted manually to fit the filaments. Length measurements were recorded on a spreadsheet and then plotted using Matlab custom functions. Means were also computed using custom Matlab functions. Only segments with 2 or 3 colors were recorded.

3.8 Supplementary Material

3.8.1 Strains used

Strain number	Relevant genotype	Reference
TH6232	Δ*hin-5717* ::FRT	Lab collection
TH9671	Δ*hin-5717* ::FRT *fliC6500*(T237C)	Lab collection
TH10548	Δ*fliO6708*(ΔAA6-121)	Lab collection
TH16123	*ΔflgM5628* ::FRT Δ*fliO6708* P*flhDC7460* Δ*hin-5717* ::FCF	This study
EM800	Δ*flgM5628* ::FRT Δ*fliO6708* P*flhDC7460* Δ*hin-5717* ::FCF *fliC6500*(T237C)	This study
EM808	Δ*araBAD1005* ::FRT	This study
EM1281	*flgM5628* ::FRT *fliO6708* P*flhDC7460* *hin-5717* ::FCF *fliC6500*(T237C) *araBAD1104* ::*flgL-bla*(100aa)	This study
EM1282	*flgM5628* ::FRT *fliO6708* P*flhDC7460* *hin-5717* ::FCF *fliC6500*(T237C) D*araBAD1099* ::*flgM-bla*	This study
EM2011	*hin-5717* ::FRT *fliC6500*(T237C) *araBAD1005* ::FRT	This study

Table 3.1 – *S. enterica* serovar Typhimurium LT2 strains used in this study

3.8.2 Scatter plots EM1281/1282

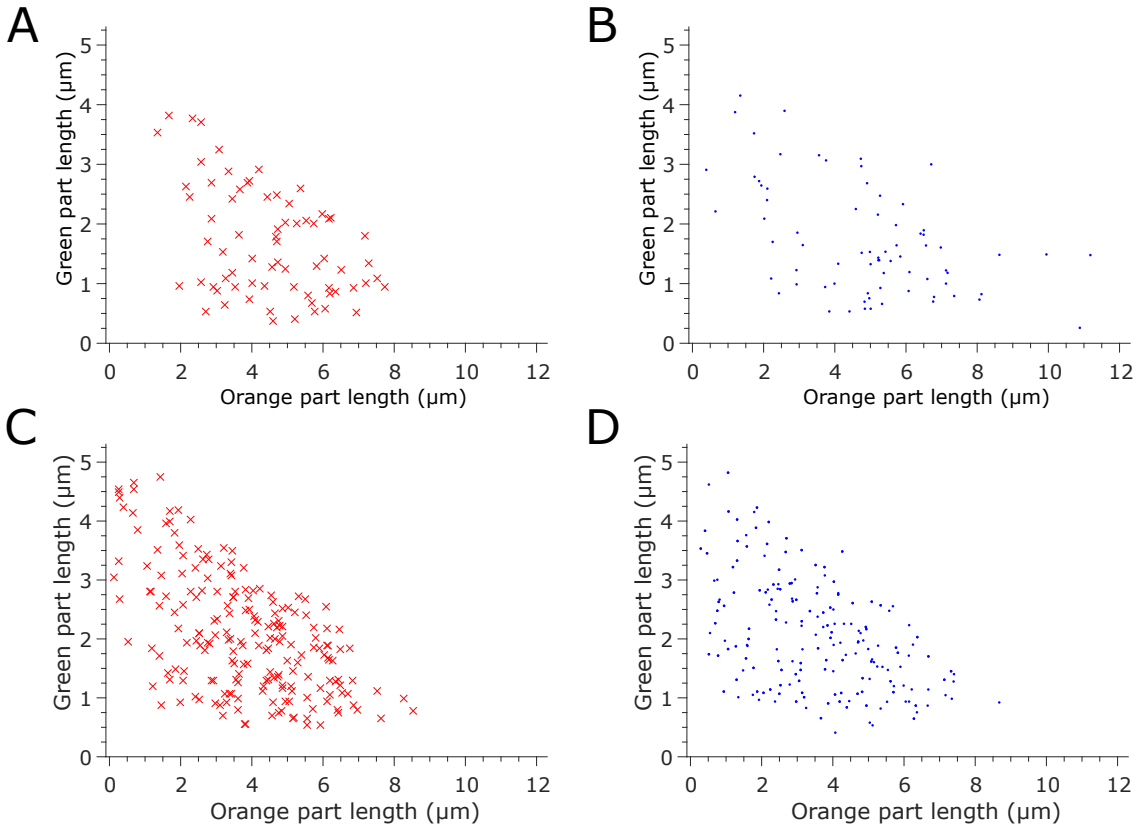

FIGURE 3.5 – Scatter plots of filaments length for strains EM1281/1282 with and without the promoter arabinose. Red 'x' markers represent filaments without the presence of arabinose and blue '.' markers represent filaments with the presence of arabinose. A and B show data for the EM1281 strain while C and D show data for EM1282 strain.

3.8.3 EM2011 strain results in the presence of arabinose

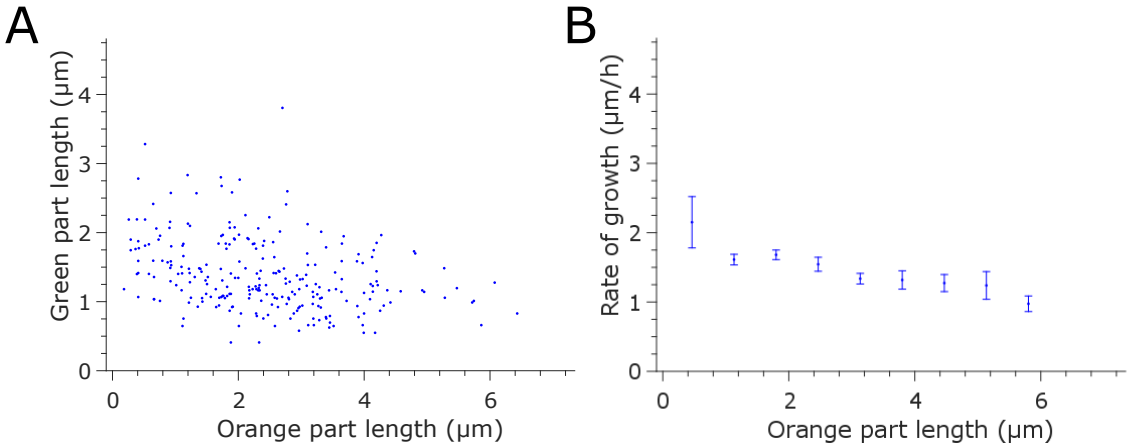

FIGURE 3.6 – Rate of growth of filaments in EM2011 strain in the presence of arabinose. Filaments were measured and graphed in A. The mean of bins obtained the same way as the EM800 strain was computed and graphed in B to show the decline in rate of growth. The error bars are the standard deviation of the distribution of each bin.

3.8.4 EM2011 strain results with only 2 labelings

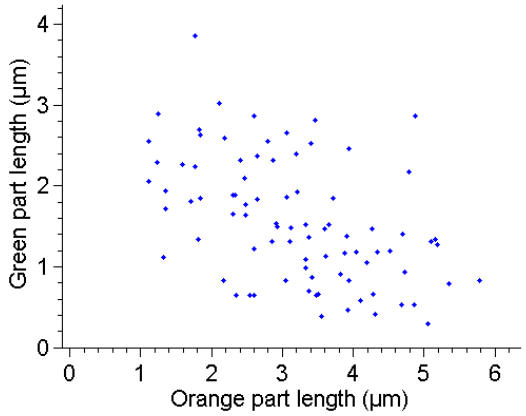

FIGURE 3.7 – Scatter plot for filaments used in the triple labeling assay not showing a third part. The strain EM2011 was used.